Seismicity Monitoring of Proppant Squeeze Operation at the Wressle W-1 Well

August 2021

Report Commissioned by Egdon Resources U.K. Limited

Report Internal ID: OLG.EG-W2-SM

Authors:
Dr. James Verdon, Lead Geophysicist, Outer Limits Geophysics LLP
Prof. Michael Kendall, Lead Geophysicist, Outer Limits Geophysics LLP
Dr. Tom Kettlety, Contract Geophysicist, Outer Limits Geophysics LLP
Dr. Antony Butcher, Contract Geophysicist, Outer Limits Geophysics LLP

SUMMARY

- This report documents the seismicity monitoring deployed in accordance with the Hydraulic Fracture Plan in order to mitigate any induced seismic events occurring during the proppant squeeze operation conducted at the Wressle W-1 well in July 2021.

- An array of five monitoring stations was deployed around the well site in local farmland. These stations provided live data streams relayed to a central processing cabin, where automated and manual processing of the data was conducted to provide real-time information about any earthquakes occurring near to the active well.

- Real time data was provided from array deployment on the 12th/13th of July until the completion of the proppant squeeze on the 25th July, except for a short period on the morning of the 25th July when the live uplink for real time data failed. Data recorded during this period was available for analysis in post-processing. Archived data was available from deployment until the decommissioning of the array on the 16th August, except for station WRE1, which experienced a power failure on the 8th August. The latency of the array was such that monitoring performance was not lost or compromised due to the failure of a single station.

- Noise levels at the five stations were low. Typical noise levels were found to range between 1×10^{-8} to 1×10^{-7} m/s, significantly below the high and moderate noise cases assumed during array design and submitted as part of the HFP. These low levels of noise mean that the array was able to meet the HFP requirements of detecting all M ≥ 0.0 earthquakes at the site, should they have occurred.

- A presumed quarry blast from the Melton Ross quarry, approximately 10 km to the east of the array, was detected on the 25th of July. A natural earthquake near to Keelby, approximately 17 km to the SE of the array, was detected on the 8th of August. These events are of no operational significance to the Wressle well, though they serve as a useful demonstration of the operational effectiveness of the monitoring array.

- No induced seismic events were detected either during the pumping operations on the 24th/25th July, or in the 20-day period following the operation. This observation is consistent with the seismic hazard assessment provided by Outer Limits as part of the HFP, which found a 90% probability that no events larger than M 0.0 would be caused by the proposed operations.

Copyright Statement

1. Introduction

Egdon Resources U.K. Limited, (Egdon), conducted a proppant squeeze operation in the Wressle W-1 well in July 2021. Egdon's Hydraulic Fracture Plan (HFP), as approved by the Oil and Gas Authority and the Environment Agency, required that real time seismicity monitoring was available to operate a Traffic Light Scheme (TLS), whereby operations would be paused or stopped if induced earthquakes larger than certain magnitude thresholds were detected. A specific condition of the OGA's consent for Egdon to undertake its proppant squeeze was, that if an Amber or Red TLS event (greater than 0.0 ML) is detected during the injection, a 24-hour period free of any further TLS events detected must lapse before the injection can re-commence.

In order to operate the TLS, a seismicity monitoring array was deployed around the wellsite, providing real-time data in order to detect, locate and characterise any seismic activity in the local area. This array was installed approximately 1 week before the start of proppant squeeze activities and was decommissioned 20 days after the cessation of operations. This report describes the seismicity monitoring at the W-1, summarising the monitoring performance of the array, and detailing what seismic activity was identified.

In Chapter 2 we describe the deployment of the array, provide details of the automated seismic processing algorithms used to detect events. In Chapter 3 we provide an assessment of the noise levels at each station, from which the detection threshold of the array can be determined. In Chapter 4 we document any seismicity recorded by the array during its operation.

2. ARRAY DEPLOYMENT

The seismicity monitoring array consisted of five independent monitoring stations. Each station consisted of a Güralp 3T seismometer (Güralp, 2019) with a Minimus digitizer (Güralp, 2021). The seismometers were buried by hand to a depth of approximately 50 cm, to ensure good coupling with the ground and to reduce surface noise. The digitizers were sited, along with batteries that provided the power source, in Pelicases™ placed at the surface. At some sites we elected to bury the Pelicases to minimise the visibility of the station. This decision was taken at site based on the expected accessibility of each site to passers-by.

The digitizers were connected to mobile antennae that streamed the recorded data to a central server, where the data streams could be accessed via an internet connection for real-time processing. GPS antennae were also connected to the digitizers to provide accurate timing information. At sites with buried Pelicases, the GPS and modem antennae were the only items visible at the surface.

Monitoring sites were pre-selected based on a desktop study that considered the optimum sites for array coverage, weighed against land access considerations and potential sources of local seismic noise. Final site locations were confirmed during a site walk-over conducted with the landowner on the 12th of July. Figure 2-1 provides a map of the station locations. Table 2-1 provides details for each station. Figures 2-2 – 2-6 show the deployment at each site.

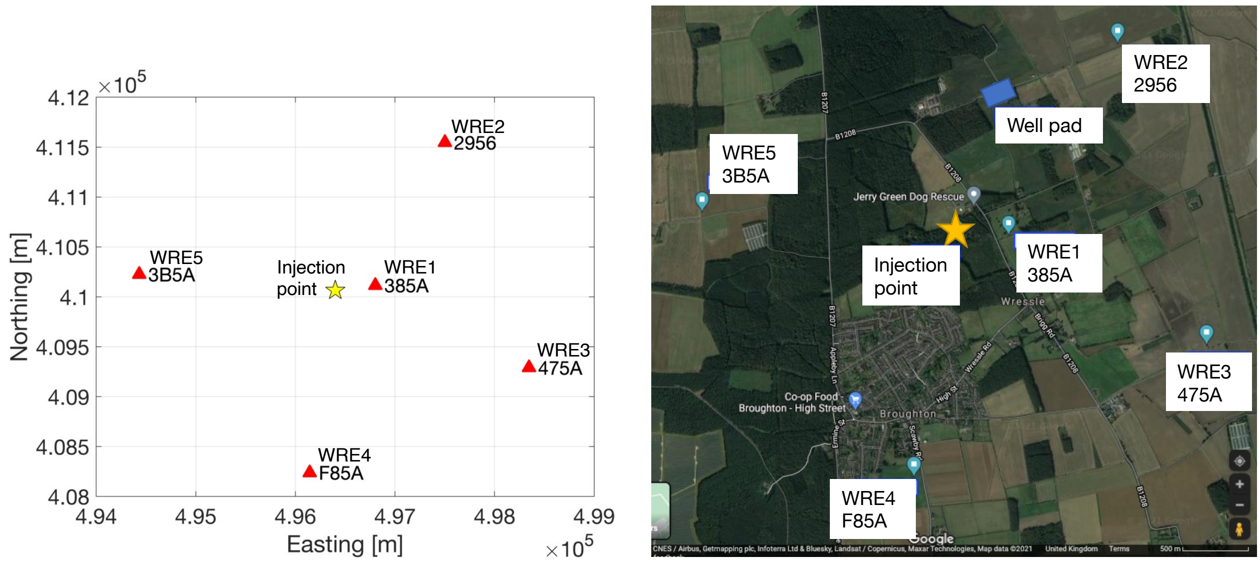

(a) (b)

Figure 2-1: Monitoring array locations. In (a) we show the positions of the monitoring stations in UK National Grid coordinates. In (b) we overlay the station positions on a Google Earth image. We also show the position of the injection point (yellow star) through which the proppant squeeze was conducted.

Table 2-1: Seismicity array monitoring station details.

	Inst. ID #	Deployed	Decommissioned.	Latitude [°]	Longitude [°]	Elev [m], AMSL
WRE1	385A	12/07	08/08	53.58	-0.54	11.7
WRE2	2956	12/07	16/08	53.59	-0.53	0.1
WRE3	475A	13/07	16/08	53.57	-0.51	7.3
WRE4	F85A	13/07	16/08	53.56	-0.55	41.7
WRE5	3B5A	13/07	16/08	53.58	-0.57	61.6

(a)

(b)

Figure 2-2: Deployment of Station WRE1. In (a) we show the buried seismometer, and in (b) we show the Pelicase containing batteries and digitizer. The GPS aerial and mobile modem were attached to an adjacent fence post.

Figure 2-3: Deployment of Station WRE2. The position of the buried seismometer is visible in the foreground, with the Pelicase containing batteries and digitizer behind. The GPS aerial and mobile modem were attached to a short length of scaffold pole.

Figure 2-4: Deployment of Station WRE3. The position of the buried seismometer is visible to the left, adjacent to the vegetation, with the Pelicase containing batteries and digitizer in the centre. The GPS aerial and mobile modem were attached to a short length of scaffold pole.

(a)

(b)

Figure 2-5: Deployment of Station WRE4. In (a) we show the seismometer in place before being covered (right), and the batteries and digitizer are visible in the open Pelicase. In (b) we show the completed station – at this site the Pelicase was also covered with earth: the GPS aerial and mobile modem attached to a short length of scaffold pole were the only objects visible at the surface.

(a)

(b)

Figure 2-6: Deployment of Station WRE5. In (a) we show the open Pelicase and antennae – the seismometer is buried at the edge of the crop field, behind the operative. In (b) we show the completed station – at this site the Pelicase was also covered with earth: the GPS aerial and mobile modem attached to a short length of scaffold pole were the only objects visible at the surface.

2.1 Data Availability

Figure 2-7 shows a timeline of data availability from all stations. All stations were deployed on the 12th – 13th of July, with real time data being available immediately after deployment of each station. An instrument fault at Station WRE1 (385A) was repaired overnight on the 13/14th July. For a short period (10:24 – 12:29) on the morning of Sunday 25th July, real time data streaming was lost due to a server fault, however this fault was remedied before operations were carried out. Real-time data transmission was disabled after completion of the main proppant squeeze operation on afternoon of the 25th of July. Archived (post-processed) data is available from this time until the decommissioning of the array on the 16th of August. Upon decommissioning of the array, it was discovered that a power failure had occurred at Station WRE1 at 1am on the 8th of August, and as such this station did not record any data after this time. It should be noted that the array was designed with a degree of latency such that the loss of one station would not affect performance, and therefore the loss of WRE1 after the 8th of August would not have affected our ability to detect induced seismicity at the Wressle site.

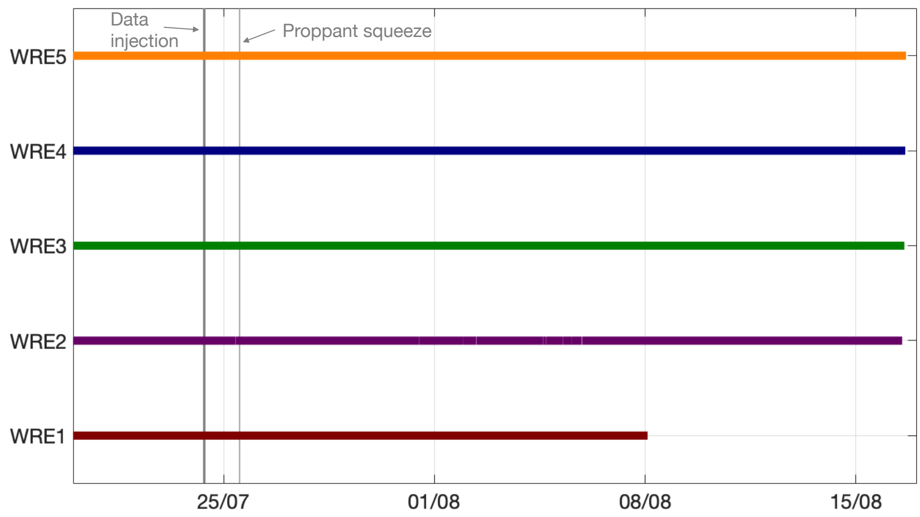

Figure 2-7: Timeline of data availability from each station, from the 19th of July onwards. The timings of the data injection and main proppant squeeze operation in the W-1 well are shown by the vertical grey lines. Data was recorded at all sites until the 8th August, when a power failure occurred at WRE1. The other four stations provided continuous data until the array was decommissioned on the 16th August.

2.2 Data Processing Workflow

Real time data was processed in the following workflow:

1. The network server was constantly scanned for new files, which were provided each minute by the data telemetry.

2. New datafiles were imported, along with 30 seconds of data from the previous period to provide overlapping time series.

3. Initial waveform processing: we detrended waveforms using a linear function, a cosine taper of length 2 % was applied, and the data were then bandpass filtered between 1.5 – 20.5 Hz. The instrument response was then removed (converting recorded units into a measurement of particle displacement in m).

4. The waveforms after initial processing were displayed for manual inspection by an OLG operative to visually identify any seismic arrivals.

5. A commonly used automated triggering algorithm was applied to the processed waveforms for event detection. This was done using the Z-detector (Withers et al., 1998) with a threshold ratio of 3.0, computed over a window length of 2 seconds. A minimum of 3 co-incident triggers at different stations was required to identify a potential seismic event. When triggered, 15-second SAC (Helffrich et al., 2013) files, centred on the trigger time, were generated for further manual analysis.

Archived data was re-processed using a similar workflow. All traces were detrended and filtered between 1.5 – 20.5 Hz, and the instrument response removed. An automated triggering algorithm (FilterPicker, Lomax et al., 2012) was then used to scan the traces for events.

In the following chapter we provide an assessment of the array detection performance based on measured background noise levels. We then discuss recorded events in Chapter 4.

3. Noise Levels and Array Performance

The requirement for the seismic monitoring array was that it should be capable of detecting all events with magnitudes greater than M 0.0, in order to operate the Traffic Light Scheme effectively. In Egdon's HFP, we performed a synthetic study to simulate the array performance and event detectability. This study examined two different noise cases – moderate noise at 1×10^{-6} m/s, and high noise at 3×10^{-6} m/s. Our study found that, even in the high noise case, the array would be capable of detecting events of magnitude M 0.0 that had a signal amplitude 1 standard deviation below the mean expected for an event of this size.

Preliminary noise analysis conducted prior to the start of the proppant squeeze indicated that noise levels at all stations were satisfactory, and no further noise mitigation or station re-siting would be required. In this chapter we further analyse the background noise levels during the proppant squeeze in order to confirm that the array was able to perform as designed with respect to event detection.

We perform our noise tests on a subsection of data, consisting of 100 minutes of recording from 12:00 (UTC, Coordinated Universal Time) on the 25th of July. This time period covers the time when pumping of the proppant squeeze was active. The raw data traces over this period are shown in Figure 3-1.

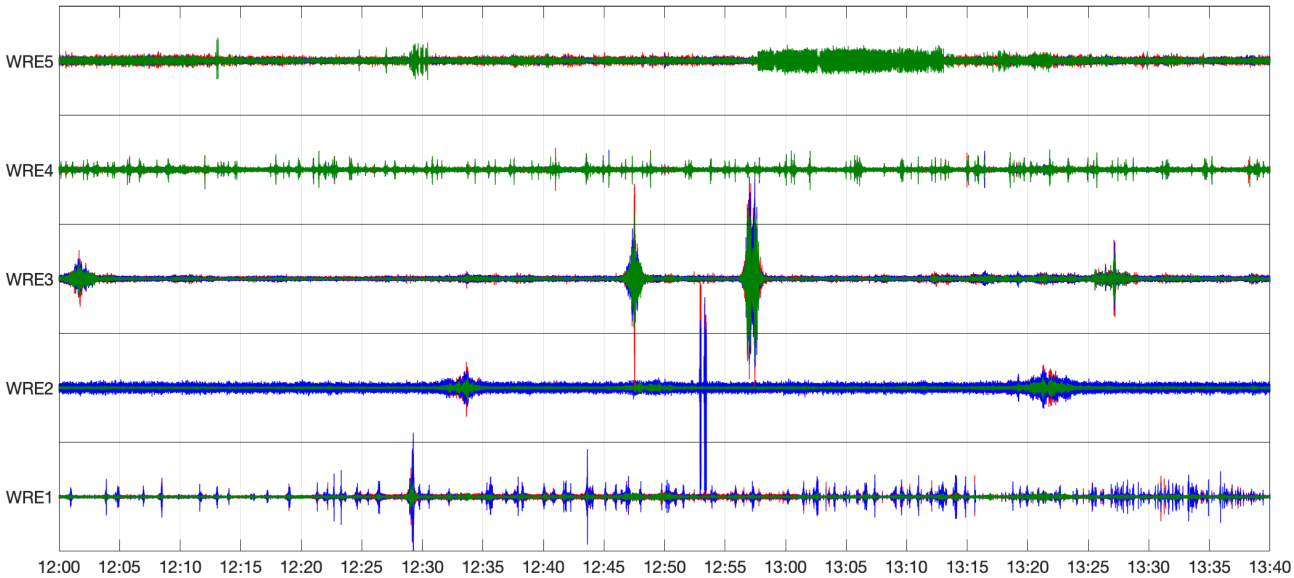

Figure 3-1: Seismograms from all 5 stations from 12:00 on the 25th July. The proppant squeeze operation ran from approximately 12:20 – 13:00 (UTC). These traces were used for the noise analysis presented in the following figures.

For our noise analyses, we divided these traces into 100 1-minute segments. For each 1-minute segment, we computed the particle velocity amplitude spectra for each component of each trace. The resulting spectra are shown in Figure 3-2. We find that amplitudes range between 1×10^{-9} to 1×10^{-6} m/s, with the overwhelming majority of values falling between 1×10^{-8} to 1×10^{-7} m/s. Figure 3-2 shows that the observed amplitudes are relatively flat between 2 – 15 Hz. To further quantify the observed noise, we consider the distribution of amplitudes at a frequency of 10 Hz, which is at the centre of the bandpass used to filter the data in our processing workflow.

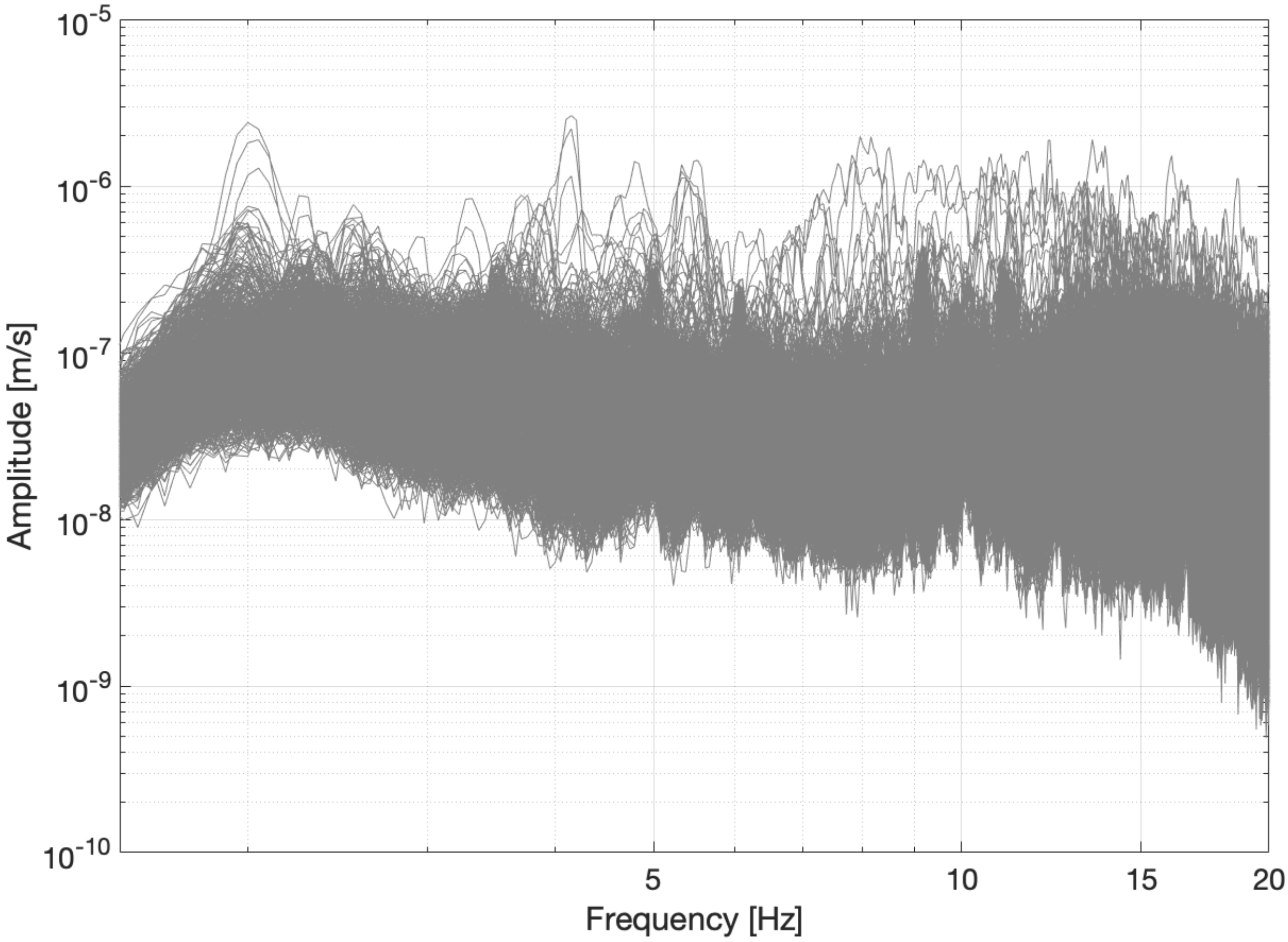

Figure 3-2: Particle velocity spectral amplitudes for each 1-minute section of traces from each component at each station.

Figure 3-3a shows the distribution of particle velocity amplitudes at 10 Hz, and Figure 3-3b shows the cumulative distribution, expressed as a percentage. We find that 95 % of the observed noise levels fall below 1 x 10^{-7} m/s, and 100 % of the observed noise levels fall below 1 x 10^{-6} m/s. As such, the noise levels recorded by the array during the proppant squeeze operation are significantly below the moderate noise case used to assess event detectability in the HFP. The monitoring array has therefore met the stipulations described in the HFP in terms of event detection capability and would have been able to detect any M ≥ 0.0 events had they occurred.

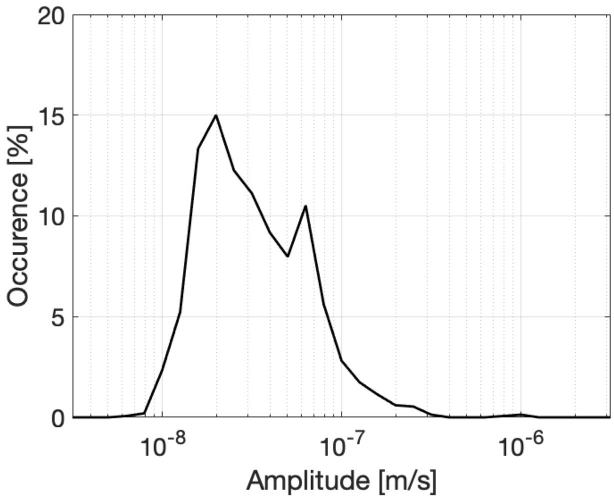

(a)

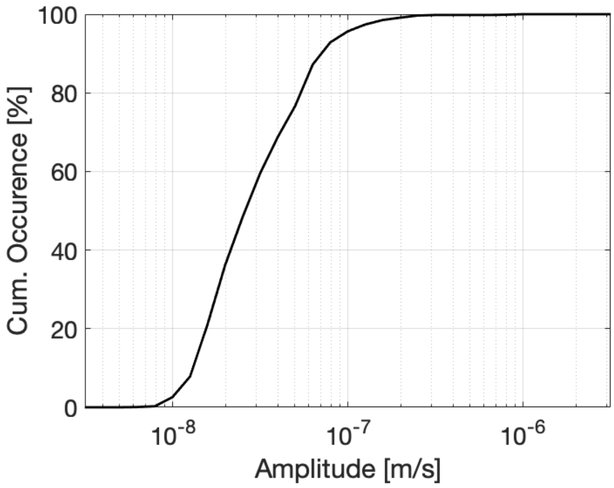

(b)

Figure 3-3: In (a) we show the distribution of observed particle velocity amplitudes at a frequency of 10 Hz during the noise analysis period. In (b) we show the cumulative distribution of particle velocity amplitudes at 10 Hz.

4. Event Detection

In this chapter we summarise the seismicity detected by the array during the monitoring period. Figure 4-1 shows the seismometer traces during the main proppant squeeze operation, scaled such that an M 0.0 event would fill the y-axis for each station. Local noise spikes are marked on individual traces, but it is clear that no earthquakes were detected. Similarly, both the real-time automatic triggering algorithm and the post-processing analysis did not identify any earthquakes during either the data frac (on the 24th of July) or the main proppant squeeze (on the 25th of July).

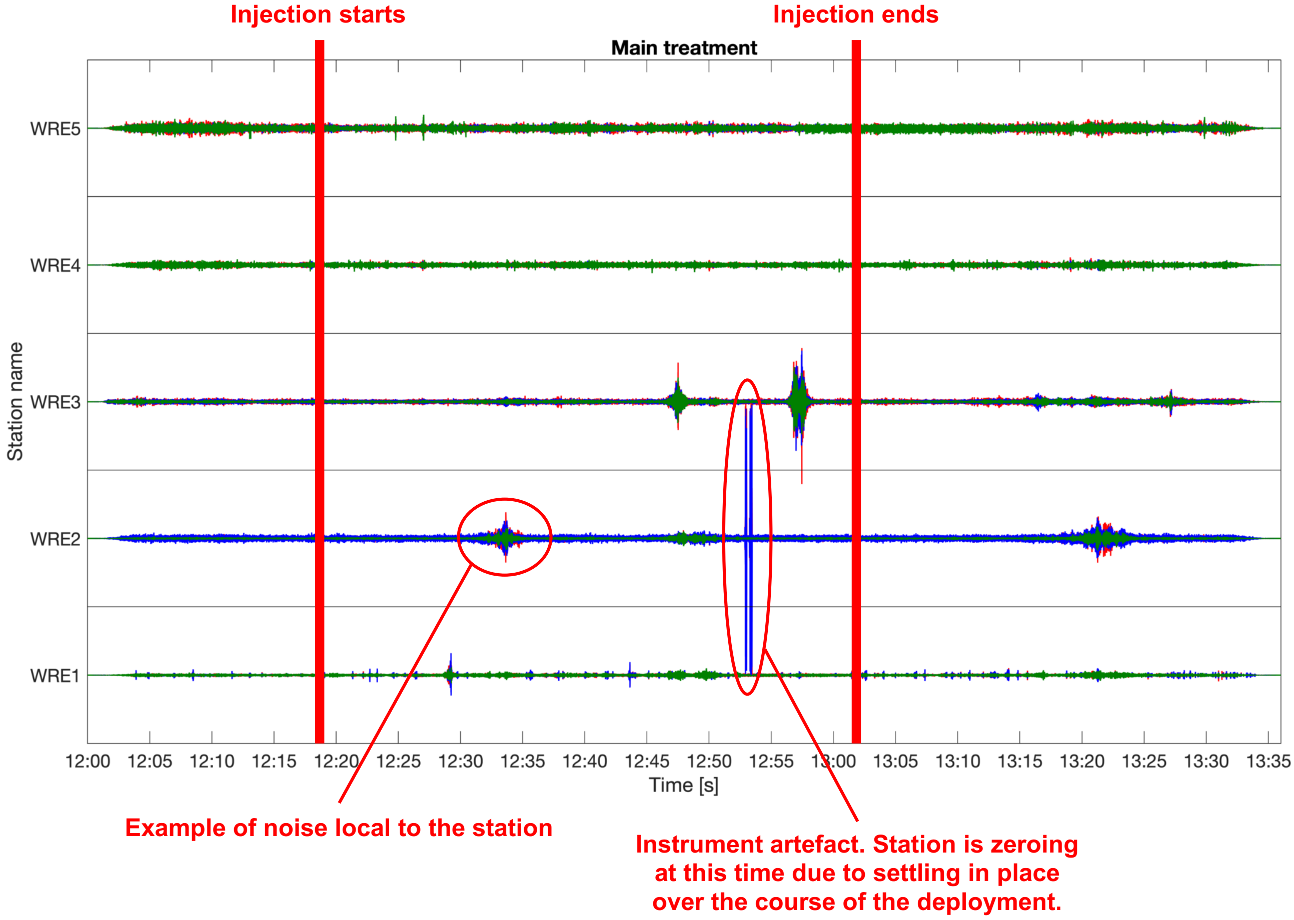

Figure 4-1: Seismograms during the main proppant squeeze operation, scaled such that an M 0.0 event would fill the y-axis for each station. The start and end of the treatment are marked, as are local noise spikes at each station. No earthquakes are visible during the injection period.

A trigger on the 25th of July at 07:26 am (UTC) was identified both during the real time processing and in post processing. The waveforms from this event are shown in Figure 4-2. The emergent nature of the S-waves is more commonly associated with surface blasts rather than earthquakes. The moveout across the array and the time separation between the P- and S-wave arrivals are consistent with a source located at the surface between 5 – 10 km to the east of the array (although the location is uncertain given the emergent nature of the S-wave arrivals). The Singleton Birch Melton Ross quarry is located at a distance of 10 km to the east of the Wressle site, and our presumption therefore is that these waveforms represent a blast conducted at this quarry.

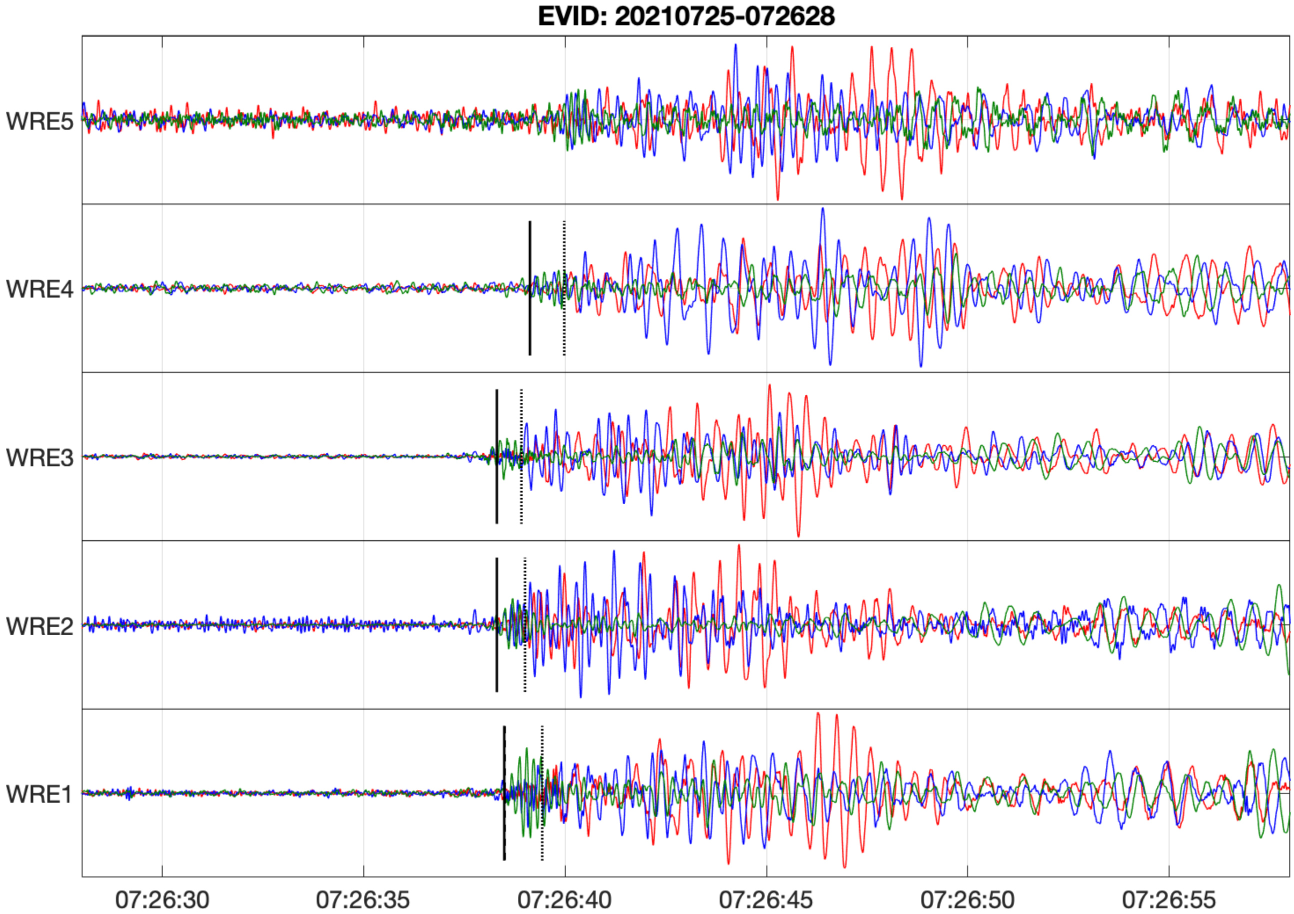

Figure 4-2: Seismograms from the presumed blast originating at the Melton Ross quarry, approximately 10 km to the east of the Wressle site. P- and S-wave picks are shown by the solid and dashed vertical lines.

A second event was observed on the 8th of August at 03:21 am. The waveforms from this event are shown in Figure 4-3. This event was also detected and located by the BGS national seismic monitoring array. The BGS located this event at a Lat/Lon of 53.55°/-0.27°, near to the village of Keelby, and at a depth of 23 km, and assigned a magnitude of M 1.7. Our observations are consistent with this location and magnitude. The epicentre of this event is therefore approximately 17 km from the Wressle site. Given the distance and depth of the event, it is clearly not induced. It has been similarly categorised as a natural earthquake by the BGS. Earthquakes of this magnitude are not uncommon in the North Lincs. region (see the seismic hazard assessment provided in the Egdon HFP).

While these events are of no operational relevance to the Wressle well, they serve as a useful means to highlight the operational effectiveness of the monitoring array.

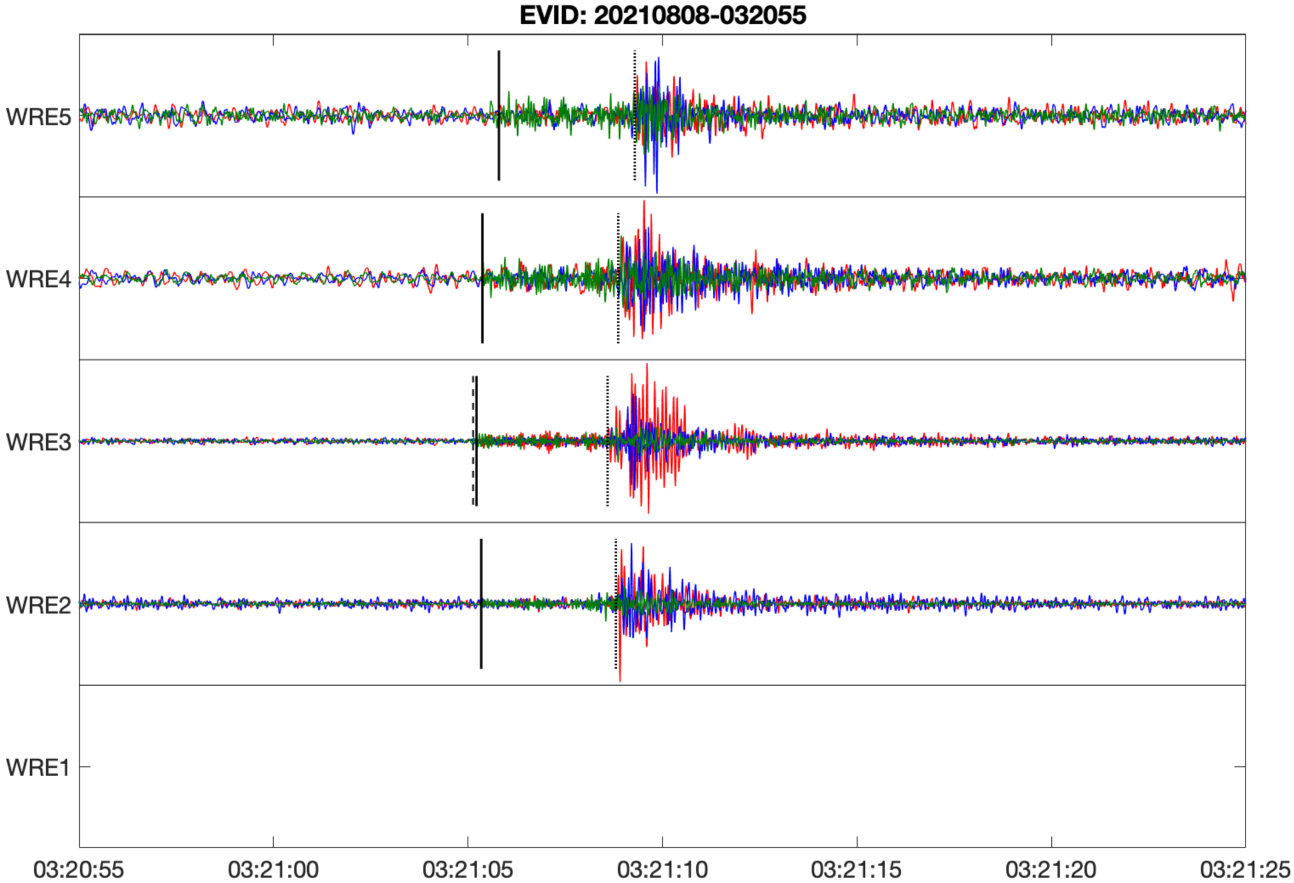

Figure 4-3: Seismograms from the Keelby earthquake on the 8th of August, approximately 17 km to the southwest of the Wressle site.

As such, we conclude that no induced events were detected by our monitoring array during or after the proppant squeeze at the Wressle W-1 well. This result is consistent with the seismic hazard assessment performed by Outer Limits as part of Egdon's HFP, where we found a likelihood of more than 90 % that no events with M > 0.0 would be caused by the proposed operation.

REFERENCES

Güralp, 2019. Güralp 3T Operator's guide. Accessed at https://www.guralp.com/documents/MAN-030-0001.pdf on 16/08/021.

Güralp, 2021. Güralp Minimus and Minimus+, Technical Manual. Accessed at https://www.guralp.com/documents/MAN-MIN-0001.pdf on 16/08/2021.

Helffrich, G., J. Wookey, I. Bastow, 2013. The Seismic Analysis Code, A Primer and User's Guide: Cambridge University Press, 173pp.

Lomax, A., C. Satriano, M. Vassallo, 2012. Automatic picker developments and optimization: FilterPicker—A robust, broadband picker for real-time seismic monitoring and earthquake early warning: Seismological Research Letters 83, 531-540.

Withers, M., R. Aster, C. Young, J. Beiriger, M. Harris, S. Moore, J. Trujillo, 1998. A comparison of select trigger algorithms for automated global seismic phase and event detection: Bulletin of the Seismological Society of America 88, 95-106.

OUTER LIMITS